energies

MDPI

Article

Influence of Temperature and Residence Time on Torrefaction Coupled to Fast Pyrolysis for Valorizing Agricultural Waste

Angel Alcazar-Ruiz, Fernando Dorado and Luz Sanchez-Silva *

Department of Chemical Engineering, University of Castilla-La Mancha, Avda. Camilo José Cela 12, 13071 Ciudad Real, Spain; angel.alcazar@uclm.es (A.A.-R.); fernando.dorado@uclm.es (F.D.)
* Correspondence: marialuz.sanchez@uclm.es

Abstract: Torrefaction is a promising pretreatment technology for valorizing biomass and upgrading pyrolysis products. This study sets out an original procedure consisting of subjecting the biomass to torrefaction before fast pyrolysis to increased value-added compounds based on agricultural waste biomasses production. This study uses a combined biomass treatment consisting of torrefaction (280–320 °C) and subsequent fast pyrolysis (500 °C) using the same reactor. Under different torrefaction temperatures and residence times, olive pomace (OP) and almond shell (AS) have been evaluated. The study demonstrated OP rather than AS was thermally unstable. The highest total yield of carboxylic acids (mainly acetic acid) was obtained by means of torrefaction at 280 °C with a residence time of 20 s for OP, and at 300 °C and 20 s for AS. Higher torrefaction temperature and residence time promoted phenolic compounds production for OP. However, OP had a higher lignin content and inherent metals that promoted a catalytic reaction during the procedure. The highest yield (47.7%) was obtained using torrefaction at 320 °C with a residence time of 240 s. Overall, the torrefaction of biomass combined with fast pyrolysis constituted a very simple and efficient strategy for valorizing the conversion of agricultural waste biomass into value-added chemicals.

Keywords: torrefaction; temperature; residence time; fast pyrolysis; olive pomace; almond shell

Citation: Alcazar-Ruiz, A.; Dorado, F.; Sanchez-Silva, L. Influence of Temperature and Residence Time on Torrefaction Coupled to Fast Pyrolysis for Valorizing Agricultural Waste. *Energies* **2022**, *15*, x. https://doi.org/10.3390/xxxxx

Academic Editor: Antonio Zuorro

Received: 22 September 2022
Accepted: 23 October 2022
Published: date

1. Introduction

As a natural carbon-neutral fuel, biomass is an ideal alternative to fossil fuels [1]. Biomass has attracted interest from researchers over the past few decades, in order to produce sustainable, environmentally-friendly fuels [2]. Currently, biomass is the largest known renewable source of energy with a global production of 220 billion tons/year. However, it is projected that lignocellulosic biomass could supply approximately 15–50% of global primary energy requirements by 2050 [3]. Among other approaches for converting biomass to energy, fast pyrolysis of lignocellulosic biomass waste has been considered one of the most promising technologies for sustainable production of liquid fuels and value-added chemicals [4]. Fast pyrolysis is defined as a thermal decomposition process carried out at a moderate temperature, a high heating rate, a short vapor residence time, and an inert atmosphere to maximize yields of bio-oil [5]. The bio-oil obtained from biomass in the procedure is a complex mixture of oxygenates, such as C1-C4 light oxygenates, carbohydrates, furans, anhydrosugars, and phenols [6]. Final end product characteristics depend upon operating parameters, such as reaction temperature and residence time [7]. Previous studies have dealt with the valorization of organic wastes through fast pyrolysis. Dorado et al. [8] determined the optimum conditions varying the effect of the operational conditions (temperature, heating rate, and vapor residence time) on fast pyrolysis product distribution of different olive pomace feeds. The olive pomace results determined not only their chemical composition, but also that their fat content has a remarkable effect on bio-oil product distribution after pyrolysis. Gonzalez et al. [9] investigated

Comentado [M1]: Notes for Authors
1. The initial layout for your manuscript was done by our layout team. Please do not change the layout, otherwise we cannot proceed to the next step.
2. Please do not delete our comments.
3. Please revise and answer all questions that we proposed. Such as: "It should be italic"; "I confirm"; "I have checked and revised all."
4. Please directly correct on this version.
5. Please make sure that all the symbols in the paper are of the same format.
6. Please note that at this stage (the manuscript has been accepted in the current form), we will not accept authorship or content changes to the manuscript text. Further updates after publication should be carefully considered.

Comentado [M2]: Please carefully check the accuracy of names and affiliations.

Comentado [ÁAR3R2]: I Confirm

Comentado [M4]: This is an important note to let you know that to protect the privacy of the author's contact information, we will only display the corresponding authors' contact information on the published paper. However, we hope the contact information of the other authors can also be confirmed or corrected during the proofreading stage, which will be recorded in our database to furnish the author's integrated publication history and also contribute to our future communications. we will only display the corresponding authors' contact information on the published paper after 4 August

Comentado [ÁAR5R4]: I Confirm

Comentado [M6]: Please check all author names carefully.

Comentado [ÁAR7R6]: I Confirm

pyrolysis of almond shells' varying temperature range (300–800 °C) and heating rates (5–20 °C/min). Bio-oil components were obtained in the range temperature (400–500 °C), being mainly found rich in hydroxyl and carbonyl compounds, and aliphatic and aromatic hydrocarbons. It can be found that the thermal degradation of biomass, such as fragmentation and depolymerization, depend on reaction temperatures [10]. The complex compositions of obtained bio-oil limit its use directly for further upgrades and refining. However, bio-oil can be upgraded to produce several bio-based chemicals that could have a variety of uses in many industries, such as biochemicals (e.g., phenolics and ketones) to be used as fine chemicals in the pharmaceutical industry, resin manufacturing, and food processing [11,12]. Therefore, various pre-treatments prior to pyrolysis can boost the production of several value-added chemical feedstocks. Thus, producing bio-phenols from varieties of biomass feedstocks is an important approach to alleviate the fossil energy crisis, due to traditional synthesis of phenol coming from the cumene process, which leads to a large consumption of fossil fuels and environmental pollution [13,14].

Lignocellulosic biomass is known to be typically composed of three main components (cellulose, hemicellulose, and lignin) together with a small amount of extractives, metals, and ash [4]. They are very different in chemical structure, which determines its reaction and product distribution under fast pyrolysis. Studies have reported that pure cellulose, hemicellulose, and lignin decomposed at different temperature ranges. Hemicellulose decomposed at a lower temperature range (210–320 °C) than pure cellulose (300–390 °C), while lignin, with the highest stability, did so at a broad range (200–550 °C) [4,15,16]. Hence, controlled pretreatment (such as torrefaction) before fast pyrolysis has been proposed as a solution for fully valorizing biomass with different operational parameters. Torrefaction is commonly known to be a thermochemical pre-treatment technique for biomass, performed under an anoxic environment at a temperature range of 200–300 °C [17]. However, at lower torrefaction reaction temperatures, decomposition rates of cellulose and lignin could lead to an evident reduction, which could limit the complete conversion of cellulose and lignin fractions within biomass [4]. Thus, it was found that most hemicellulose and part of lignin fractions were first decomposed during torrefaction. Therefore, torrefied biomass can be further converted into a rich biochemical bio-oil via fast pyrolysis [18]. Several studies on torrefaction pre-treatment followed by pyrolysis concluded that the physicochemical characteristics of the biomass and biofuel produced were superior to those of raw biomass [2,17,19]. In this regard, Chen et al. [10] analyzed the thermodegradation of hemicellulose, cellulose, and lignin behavior over torrefaction, pyrolysis, and their combination. Torrefaction was observed to be a determinant of lignin pyrolysis decomposition. Zhen et al. [20] studied a two-stage controllable pyrolysis process of biomass based on torrefaction and subsequent fast pyrolysis of impregnated eucalyptus. Nepal et al. [21] researched the effect of torrefied temperatures on the physical and chemical transformation of spent coffee grains. The decrease in oxygen content and increase in fixed carbon content enhanced the effect of torrefaction on fuel properties, and therefore, torrefaction could upgrade feedstocks [2].

Although torrefaction and pyrolysis reactors have rapidly developed, many challenges and barriers must be overcome to maximize the production of bio-based chemicals and the financial benefits of the integrated process. As far as we know, few studies have been published on the effect of the most critical operational conditions (temperature and residence time of a prior torrefaction) during biomass feedstock valorization in a two-stage procedure, carried out in a single-step process [4,22]. This study is innovative due to carrying out both torrefaction (280–320 °C) and fast pyrolysis (500 °C) processes using the same reactor. On the other hand, olive pomace and almond shell were used as biomass waste feeds to understand how its different physicochemical properties affect bio-oil product distribution. Therefore, a thorough study on how torrefaction operating parameters (reaction temperature and residence time) influence product distribution of value-added biochemicals, such as ketones and bio-phenolics, was conducted.

2. Materials and Methods

2.1. Materials Feed and Preparation

In this study, olive pomace (OP) and almond shell (AS) were used as biomass waste feed. OP was provided by Aceites Garcia de la Cruz olive oil mil (Castilla-La Mancha, Spain), and AS was collected from Castilla-La Mancha region (Spain). The biomass sample was oven-dried for 24 h at 100 °C, and then ground and sieved to obtain an average particle size ranging from 100 to 150 μm.

Proximate and ultimate analyses were carried out to determine compositions of the studied samples (following standards UNE 15104:2011, UNE-EN ISO18123, UNE 32-004-84, and UNE 32-002-95) using the elemental analyzer Flash Smart Elemental Analyzer (Thermo Scientific, Waltham, MA, USA) equipped with a thermal conductivity detector. The proximate analysis yielded information on volatile matter, fixed carbon, and ash content. The ultimate analysis was used to find the concentrations of carbon, hydrogen, nitrogen, oxygen, and sulfur in the samples. Several studies have tried to find the correct model to predict the higher heating value (HHV) of the agricultural crop residue based on the composition of the main components (carbon, hydrogen, and oxygen) from an ultimate analysis of biomass fuels [23,24]. In this work, the HHV was calculated using an empirical HHV model applied to a wide range of data sets and fuel species (Equation (1) [25]; Table 1):

$$\text{HHV (MJ/kg)} = 0.3491\ C + 1.1783\ H + 0.1005\ S - 0.1034\ O - 0.0151\ N - 0.0211\ A \quad (1)$$

where C, H, S, O, and N are the weight percentages for carbon, hydrogen, sulfur, oxygen, and nitrogen, respectively; while A is the weight percentage for ash.

The alkali and alkaline earth metals (AAEMs) content in each sample was determined by Inductively Coupled Plasma-Optical Emission Spectrometry (ICP-OES). Here, Varian 720-ES equipment (which was previously calibrated using standard stock solutions) was used. The chemical composition (hemicellulose, cellulose, and lignin) of raw biomass waste was obtained with a Soxhlet extractor [26,27]. For OP, contents of extractives, hemicellulose, and Klason lignin were determined with the following experimental methodology due to its grassy nature [28]: First, the extractive contents were determined by extraction using the Soxhlet system successive exhaustion method using dichloromethane (6 h), ethanol (16 h), and water (16 h), as an adaptation from TAPPI 204 om-97. After extraction, the sample was dried at 110 °C for 1 h and cooled to room temperature in a desiccator. The extractives solubilized by the solvents were determined by mass differences in the solid. Lignin content was then determined by the Klason method (TAPPI T 222 om-02). The samples (350 mg) of extractive-free material were added to 3 mL of H_2SO_4 (72%) at 30 °C for 1 h, then diluted to 3% *w*/*w* H_2SO_4 and reacted in an autoclave for 1 h at 120 °C. The residue was filtered, washed until neutralization, dried at 110 °C until reaching a constant weight, and cooled to room temperature. The weight difference after treatment determined the amount of Klason lignin. For determining hemicellulose contents, 150 mL of NaOH solution (0.5 M) was added to 1 g of extractive-free material and boiled for 3.5 h with recycled water. The product was filtered, washed until neutralization, dried at 110 °C for 1 h, and cooled to room temperature. The weight difference after treatment determined the amount of hemicellulose. For AS, lignin, hemicellulose, and cellulose, the content was calculated following an experimental methodology reported elsewhere [27]. The characterization results of raw biomass wastes used in this work are listed in Table 1.

Comentado [M8]: We added the location (city, state, country) of this company, please check it.

Comentado [ÁAR9R8]: I Confirm

Comentado [M10]: We made it italic, please confirm this revision.

Comentado [ÁAR11R10]: I Confirm

Table 1. Physicochemical properties of biomass waste feed.

Sample	Proximate Analysis (wt.%) *daf				Ultimate Analysis (wt.%) *daf				HHV
	Moisture	Ash	Volatile Matter	Fixed Carbon *diff	C	H	N	O *diff	(MJ/kg)
OP	2.68	4.44	91.87	3.69	53.2	6.83	1.54	38.28	22.56
AS	5.13	2.22	92.01	5.77	45.86	5.88	0.35	47.92	17.93

Sample	Chemical composition (wt.%) *db			
	Lignin	Hemicellulose	Cellulose	Extractives
OP	24.1	27.6	-	28.9
AS	13.4	28.1	39.7	-

Sample	Mineral content (wt.%)			
	K	Ca	Na	Mg
OP	1.46	0.50	0.10	0.13
AS	0.87	0.55	0.12	0.06

*daf: dry and ash free basis; O diff: % of oxygen calculated from the difference in C, H, N, and S; Fixed carbon *diff: % in fixed carbon calculated from difference in ash and volatile matter; *db: dry basis.

2.2. Experimental Procedure

Torrefaction and fast pyrolysis of raw biomass wastes (OP and AS) were carried out in a commercial micropyrolyser (Pyroprobe 6200 pyrolysis, CDS analytical, Oxford, PA, USA) connected to a 7890B/5977B GC/MS analyzer (Agilent Technologies, Santa Clara, CA, USA) with a transfer line (length: 1 m; temperature: 340 °C).

The weight of the sample was accurately weighed on an analytical balance with an accuracy of 0.001 mg (XSR105DU, Mettler-Toledo, Switzerland). An amount of 1 mg ± 0.05 mg of raw samples were placed in the middle of a quartz tube (2 mm diameter and 20 mm long) with a quartz wool base, and were then fed into a platinum Pyroprobe autosampler. Torrefaction of raw biomass wastes was performed at different temperatures (280, 300, and 320 °C) at a heating rate of 10 °C/s and varying the residence time (20, 120, 240, and 360 s). The valve interface temperature was equivalent to the torrefaction temperature. The vapor generated from torrefaction was analyzed by GC/MS. The GC/MS injector temperature was kept at 280 °C. An Elite-35MS capillary column (30 m × 0.25 μm) was used for chromatographic separation. Helium (99.999%) was selected as the carrier gas at a constant flow rate of 1 mL/min and a 1:80 split ratio. The purpose of this was to separate the different chemicals in the bio-oil and identify them. The oven temperature was programed from 40 °C (3 min) to 280 °C at a heating rate of 5 °C/min. After that, the torrefied sample remaining inside the Pyroprobe was directly fast-pyrolyzed at 500 °C at a heating rate of 20 °C/ms for 15 s, which were the operational conditions previously optimized elsewhere [8]. Additionally, the vapor products from fast pyrolysis were analyzed by GC/MS under the same previously cited conditions. The chromatograms were integrated, and the relative peak areas were calculated and subsequently identified using the National Institute of Standards and Technology (NIST) library as a reference. Only peaks with a matching quality of over 80% were considered. As shown in Figure 1, biomass waste was first torrefied by varying reaction temperature (280, 300, and 320 °C) and residence time (20, 120, 240, and 360 s). Finally, it was fast-pyrolyzed at 500 °C as an additional step for fully converting the biomass waste in order to maximize production of the desired valuable chemical compounds.

Comentado [M12]: Please confirm if it should be changed to O *diff.

Comentado [ÁAR13R12]: No, i do not confirm that change.

Comentado [M14]: We added city and state of this company.

Comentado [ÁAR15R14]: I Confirm

Comentado [M16]: Please provide the city of this company.

Comentado [ÁAR17R16]: I do not have the exactly city, just the country of the company.

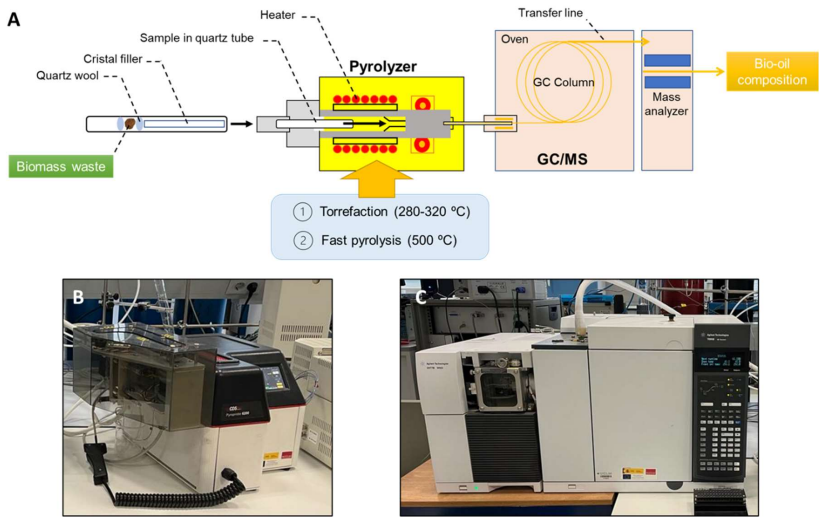

Figure 1. (**A**) Schematic flowsheet of torrefaction combined with fast pyrolysis for bio-oil production, (**B**) Pyroprobe 6200 pyrolysis, and (**C**) Agilent Technologies 7890B/5977B GC/MS.

The experiments were carried out in triplicate for each sample to ensure reproducibility. The peak area based on Py-GC/MS analysis could not reveal the real content of the target compounds. When the sample mass remained constant during each pyrolysis experiment, the corresponding chromatographs could be compared to reveal how its content had changed.

In this two-stage procedure, torrefaction and fast pyrolysis samples were denoted as *B-T-t*$_R$: where *B* is the studied biomass, *T* the temperature (°C), and t_R the retention time (s) used for torrefaction pretreatment. For example, the OP sample torrefied at 280 °C for 20 s and subsequently fast-pyrolyzed at 500 °C is denoted as OP-280-20. With direct fast pyrolysis (without torrefaction) at 500 °C, the sample was denoted as *B-500*: where B symbolizes the pyrolyzed biomass waste used. For instance, AS-500 refers to direct fast-pyrolyzed almond shell.

Comentado [M18]: Please confirm if the italics is unnecessary and can be removed. The following highlights are the same

Comentado [ÁAR19R18]: I Confirm

3. Results

3.1. Olive Pomace Torrefaction Combined with Fast Pyrolysis

Figures 2–4 show bio-oil product composition for OP at different torrefaction residence times when torrefaction temperature was set at 280, 300, and 320 °C, respectively, followed by fast pyrolysis at 500 °C. Direct fast pyrolysis of OP at 500 °C (OP-500) was denoted with a torrefaction residence time of 0. The bio-oil products were separated into functional groups: alcohols, aldehydes, alkanes, cyclic hydrocarbons, carboxylic acids, ketones, nitrogenates, phenols, and sugars. Tables S1–S3 give a detailed breakdown of the chemical composition of the bio-oil obtained in these experiments.

The compounds obtained might be related to the organic matrix of biomass, and also, to torrefaction temperature. During torrefaction, hemicellulose (which has poor thermal stability) decomposed first, and its content sharply decreased with an increase in temperature. Cellulose (which has a relatively stable structure) exhibited marginal decomposition during high-temperature torrefaction [29]. However, the lignin structure was stable, and its products were mainly degraded during pyrolysis.

Direct fast pyrolysis of OP was carried out to compare the results with and without torrefaction pretreatment. A high pyrolysis temperature and the catalytic activity of AAEMs are known to possibly lead to undesired C–C and C-O bond scissions, such as decarboxylation, decarbonylation, and ring fragmentation reactions, resulting in the formation of large amounts of non-condensable gas and C1-C4 light oxygenates [2]. The most representative group detected was phenolics from lignin decomposition, which reached a yield of 33.8%. Phenolic compounds are of great interest to society due to their antioxidative and possible anticarcinogenic activities. Dietary phenolics are considered anti-carcinogens as they are antioxidants [30]. However, conventional synthesis of phenol is carried out by cumene process, which comes from two different petroleum-based feedstocks, benzene and propene, leading to a large consumption of fossil fuels [14]. Therefore, the production of bio-phenolic compounds from a greener source, such as biomass feed, revealed an important method by which to alleviate the fossil fuel energy crises. The presence of inherent metals in OP, especially potassium (Table 1), promoted dehydration and demethoxylation reactions of lignin, which produced phenolic compounds [2,31]. A more detailed study was carried out on the phenolic compounds detected, as they were the main functional groups obtained. According to the different oxygen-containing substituted groups (hydroxyl (-OH) and methoxyl (-OCH_3)) linked to the benzene ring, the phenolics obtained were distributed into four types of components: (i) phenol type (P-type), which contains only one hydroxyl; (ii) catechol type (C-type), which contains two hydroxyls; (iii) guaiacol type (G-type), which contains one methoxyl and one hydroxyl; and iv) syringol type (S-type), which contains two methoxyl and one hydroxyl-substituted group [32,33]. From Table 2, OP fast pyrolysis at 500 °C revealed that G-type phenols were the main group. However, as observed in Figures 2–4, more value-added lignin derivates such as Guaiacol (*Phenol 2-methoxy*) and Syringol (*Phenol 2,6-dimethoxy*) were obtained after torrefaction, reaching yields of 3.8 and 5.4%, respectively. Guaiacol could be used as a model compound, i.e., a carbon-based starting material for solvents in pharmaceutical issues, as pesticide, fragrance, and in cosmetics [34,35]. On the other hand, syringol could be used in the pharmaceutical sector, in platelet aggregation, and for anti-dermatophyte activity [36]. After phenolics, carboxylic acids were the next most representative chemical compounds accounting for 20.1% of the yield. In addition, high production of acetic acid was seen with fast pyrolysis of raw OP (15%). According to the literature, high yields of acetic acid were due to large amounts of hemicellulose in the raw material (Table 1), which underwent ring scission to produce the acid [31,37]. Yields of hydrocarbon compounds were remarkable: 11.6% of cyclic hydrocarbons and 2.8% of chain olefins. Moreover, several nitrogen compounds were obtained in the form of amides, nitriles, and aromatic amines. This production is related to the nitrogen obtained from the elemental analysis (Table 1). It is predicted that nitrogenates were not altered by the catalytic effect of AAEMs [38,39].

To gain an insight into the effect torrefaction has prior to fast pyrolysis, its influence on carboxylic acid, ketones, and lignin derivates was studied and, in particular, phenolic compound yields. *Acetic acid* was selected as the representative compound for the carboxylic acids group. With ketones, *2-propanone-1-hydroxy* and *ethanone, 1-(1-cyclohexen-1-yl)* were selected as the most representative compounds. From the lignin-derived compounds, the phenolic group, value-added compounds, such as *Guaiacol, 4-methyl Guaiacol, Syringol*, and *4-(1-propenyl)* Syringol, were selected to be studied.

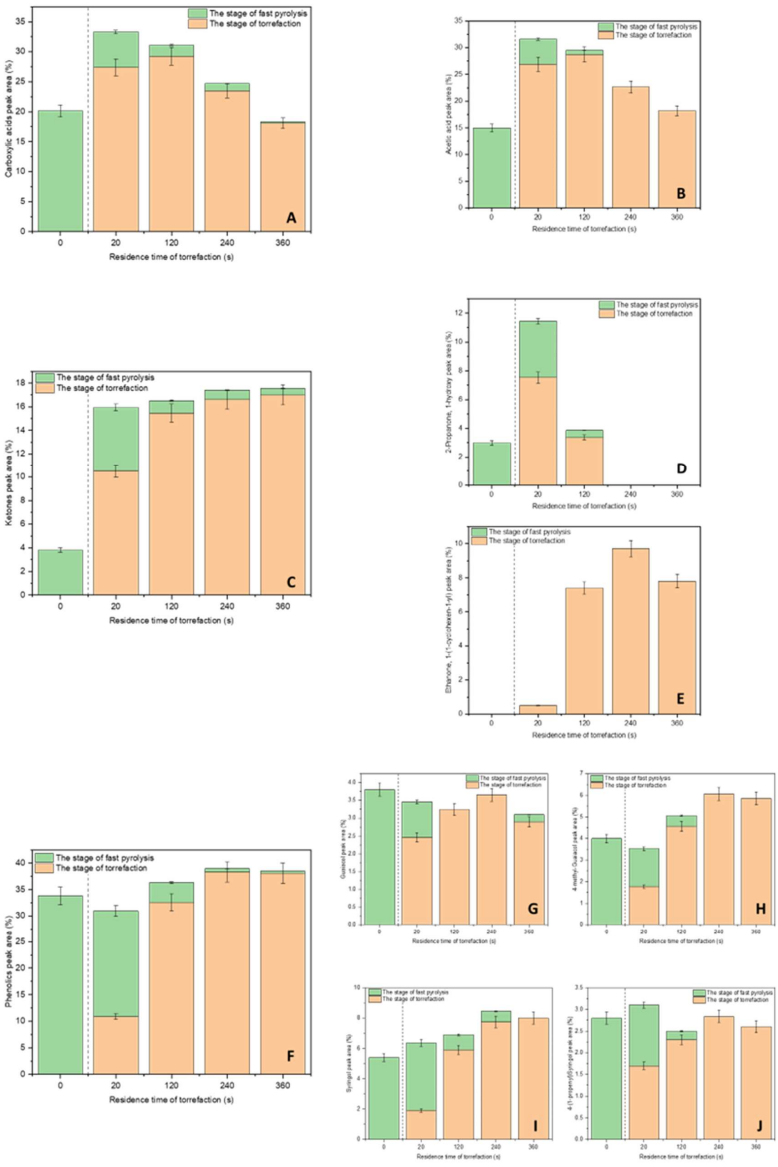

Figure 2. Bio-oil product composition for torrefaction at 280 °C and fast pyrolysis of OP. (**A**): yield of the sum of carboxylic acids, (**B**): yield of acetic acid, (**C**): yield of the sum of ketones, (**D**): yield of 2-propanone-1-hydroxy, (**E**): yield of ethanone, 1-(1-cyclohexen-1-yl), (**F**): yield of the sum of phenolics, (**G**): yield of Guaiacol, (**H**): yield of 4-methyl Guaiacol, (**I**): yield of Syringol, and (**J**): yield of 4-(1-propenyl) Syringol.

Comentado [M20]: The contents of this figure are not legible. In order to convert a clear PDF document, whilst retaining its high quality, we kindly request the provision of figures and schemes at a sufficiently high resolution (min. 1000 pixels width/height, or a resolution of 300 dpi or higher).

Comentado [ÁAR21R20]: I has been provided

As shown in Figure 2, most oxygenated compounds were produced during torrefaction. This highlights the high potential for thermal degradation of OP at low temperatures. Production of carboxylic acids was promoted at low residence times (20–240 s). Thus, yield increased from 20.1% for OP-500 up to 33.3% for OP-280-20. Interestingly, its production significantly decreased to 18.3% at the highest residence time, 360 s. This trend was attributed to the decomposition of hemicellulose into carboxylic acids at a low temperature and short residence times [40]. As observed in Figure 2B, *acetic acid* was mainly produced (which could have come from the thermal decomposition of the acetyl groups linked to the xylose compounds in hemicellulose polysaccharides). Thus, at lower torrefaction temperatures, hemicellulose decomposed, leading to an increase in the relative content of cellulose in the biomass. The removal of acetoxy- and methoxy- groups linked to the xylose units of hemicellulose reduced selectivity of carboxylic acids and increased that of ketones in the bio-oil. This phenomenon occurs because of the ketonization and rearrangement of carboxylic acids during pyrolysis of torrefied biomass [22]. As shown in Figure 2C, the formation of ketones was further enhanced at higher residence times and were mostly obtained during torrefaction. The formation of ketones comes from the deacetylation of O-acetyls and dehydration of hydroxyls in hemicellulose, as well as ring-opening of glucans in cellulose and glycosyl in hemicellulose [22,29]. Direct pyrolysis of OP produced a 3.8% yield of ketones, which reached 15% with torrefaction. Among ketonic compounds, mainly *2-propanone-1-hydroxy* (Figure 2D) and *ethanone, 1-(1-cyclohexen-1-yl)* (Figure 2E) were obtained. The former was largely produced with short torrefaction residence times, and the latter was produced with the longest. Regarding phenolic compounds, the joint procedure yielded more phenols than with direct fast pyrolysis, and its content increased with longer torrefaction residence times. This was the lignin fraction in the biomass, which was enriched with increasing torrefaction severity [40]. Production of phenolic substances was mainly due to structural changes in lignin caused by ether bond cleavage and demethoxylation [29]. During torrefaction, the cracking of hemicellulose and cellulose led to a relative increase in lignin content. As shown in Table 2, phenolics were enhanced from a 33.8% yield in direct fast pyrolysis to 38.9 and 38.5% yields for OP-280-240 and OP-280-360, respectively. These results revealed that thermal lignin decomposition in OP could be enhanced when high torrefaction residence times were used, despite the low temperature during torrefaction. Looking at this in more detail (see Table 2), G-Type compounds were enhanced in OP-280-240, specifically *4-methyl Guaiacol* (Figure 2H) with a selectivity of 6.1%, and were entirely obtained during torrefaction. For S-type compounds, *Syringol* was further enhanced to a yield of 8.4% for OP-280-240.

Comentado [M22]: Please confirm if the italics is unnecessary and can be removed. The following highlights are the same

Comentado [ÁAR23R22]: I Confirm

Comentado [M24]: There is no Figure 1H, please revise it.

Comentado [ÁAR25R24]: It has been revised, as follows: "Figure 2H"

Table 2. Bio-oil phenolic compounds distribution of torrefied and fast pyrolysis for OP.

Sample	Peak Area (%)				
	Total Phenols	**P-Type**	**C-Type**	**G-Type**	**S-Type**
OP-500	33.8	1.1	2.6	16.3	10.2
OP-280-20	30.9	0.7	1.1	17.5	10.0
OP-280-120	36.3	2.7	3.3	17.0	9.8
OP-280-240	38.9	0.0	3.7	18.4	11.6
OP-280-360	38.5	2.9	3.9	16.3	10.6
OP-300-20	23.6	0.8	0.3	14.8	6.9
OP-300-120	26.6	0.5	1.7	13.0	9.6
OP-300-240	39.4	0.9	3.6	19.3	12.4
OP-300-360	40.8	1.2	3.4	21.5	12.0
OP-320-20	30.7	0.5	0.5	17.9	11.2
OP-320-120	35.3	1.8	2.4	17.1	10.8
OP-320-240	47.4	0.6	3.5	19.7	14.9
OP-320-360	42.0	0.0	4.2	22.6	12.0

The effect of torrefaction at 300 °C combined with fast pyrolysis at 500 °C on bio-oil product distribution is shown in Figure 3.

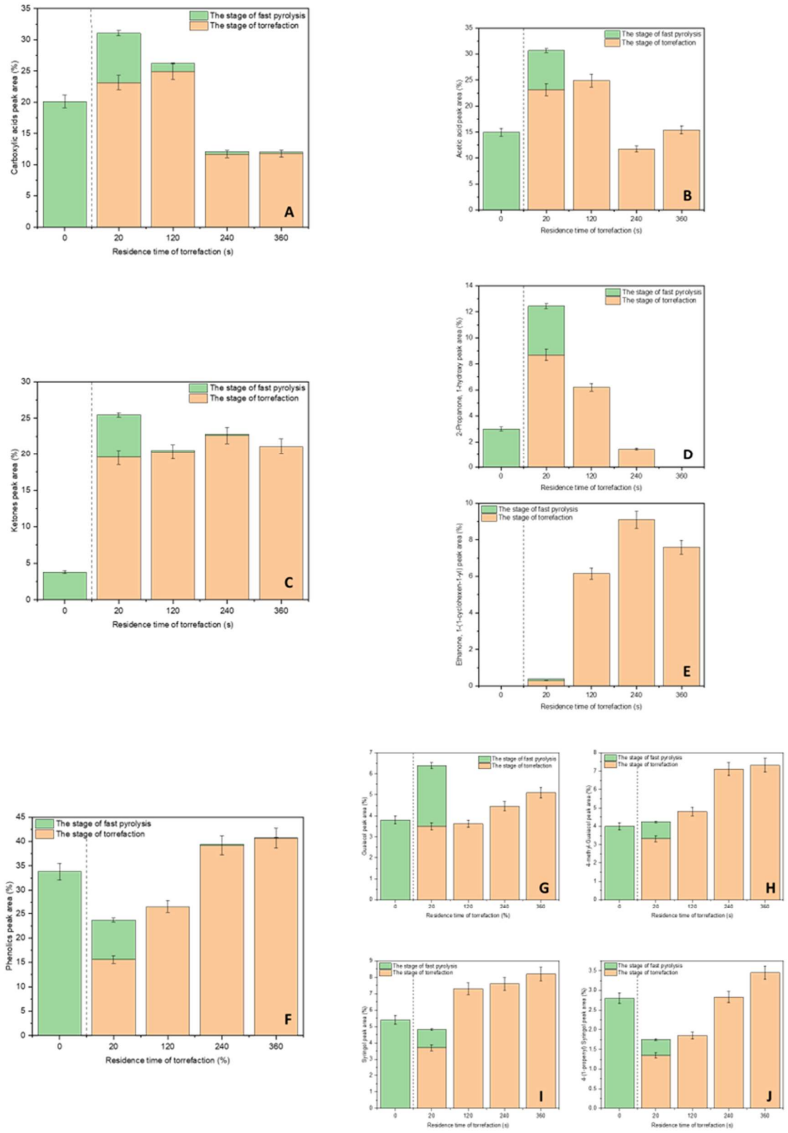

Figure 3. Bio-oil product composition for torrefaction at 300 °C and fast pyrolysis of OP. (**A**): yield of the sum of carboxylic acids, (**B**): yield of acetic acid, (**C**): yield of the sum of ketones, (**D**): yield of 2-propanone-1-hydroxy, (**E**): yield of ethanone, 1-(1-cyclohexen-1-yl), (**F**): yield of the sum of

Comentado [M26]: Please provide a clearer picture.

Comentado [ÁAR27R26]: I has been provided

phenolics, (**G**): yield of Guaiacol, (**H**): yield of 4-methyl Guaiacol, (**I**): yield of Syringol, and (**J**): yield of 4-(1-propenyl) Syringol.

As can be seen, most of the compounds detected were produced during torrefaction. However, fast pyrolysis was still significant at low torrefaction residence time (20 s). Regarding carboxylic acids (Figure 3A), they were enhanced in comparison with direct fast pyrolysis with low residence times (20 and 120 s). The increase in acids was mainly due to the production of acetic acid, as shown in Figure 3B. In comparison with torrefaction at 280 °C, a lower yield of carboxylic acids was obtained. Lower torrefaction temperatures decomposed hemicellulose, leading to an increase in the relative content of cellulose in OP. Thus, the removal of acetoxy- and methoxy- groups linked to the xylose units of hemicellulose decreased yields of carboxylic acids and increased that of ketones in the bio-oil [22]. This can be seen in Figure 3C, where a larger amount of ketones were produced than at 280 °C. Thus, the formation of ketones shot up from 3.8% (direct fast pyrolysis) to 21% for OP-300-20. This was similar to what occurred at 280 °C, the largest yield of ketones was obtained at a residence time of 20 s. From Figure 3D,E, *2-propanone-1-hydroxy* and *ethanone, 1-(1-cyclohexen-1-yl)* were the main ketonic compounds produced. The former was produced in large amounts at short torrefaction residence times (OP-300-20), and the latter at higher times (OP-300-240). During torrefaction, the cracking of hemicellulose and mild cellulose led to a relative increase in lignin content. Thus, the formation of phenolic substances was promoted at higher torrefaction temperatures and residence times. As shown in Figure 3F and Table 2, phenolics were enhanced from a yield of 33.8% with direct fast pyrolysis to 39.4 and 40.8% in OP-300-240 and OP-300-360, respectively. These results demonstrated that lignin decomposition was enhanced at high torrefaction residence times. When analyzed in more detail, G-type were the main group of phenolics obtained at 300 °C, as shown in Table 2, followed by S-type phenolic compounds. Large amounts of G-type were detected in OP-300-360 (21.5%) and the S-type in OP-300-240 and OP-300-360 (12%). Among the G-type group, guaiacol was the main compound obtained in OP-300-20 (Figure 3G), whereas *4-methyl guaiacol* was the main one in OP-300-360 (Figure 3H). They were all produced during torrefaction with a yield of 7.3%. Regarding the S-type compounds, *syringol* and *4-(1-propenyl) syringol* were the main products, with yields of 8.2% and 3.5%, respectively.

The results for a torrefaction temperature of 320 °C followed by fast pyrolysis at 500 °C are given in Figure 4.

Again, most of the components detected were produced during torrefaction. Generally speaking, the same trends were observed, confirming the previous results. Thus, as shown in Figure 4A, a greater amount of carboxylic acid compounds were obtained at low torrefaction residence times, in comparison with previous research regarding yields at low temperatures. As commented above, if torrefaction conditions become more severe, the relative content of acids significantly decreases, as acetic acid is mainly derived from deacetylation of hemicellulose which decomposes during torrefaction [32,33]. Production of ketones (Figure 4C) was mainly promoted at high residence times. As seen in Figure 4E, *ethanone, 1-(1-cyclohexen-1-yl))* followed the same previous detailed trends, with the maximum yield occurring in OP-320-360. Phenolic compound production was largely obtained in OP-320-240, reaching a yield of 47.4%, with enhanced yields of G-type (19.7%) and S-type compounds (14.9%). Among all phenolic compounds, *Syringol* (8.7% in OP-320-240) was the main compound. Interestingly, the content of phenols gradually increased with torrefaction temperature and residence time, which was logical. The phenolic compounds were derived from the thermal degradation of lignin [31], the content of which is relatively high in the organic matrix of OP (24.1 wt.%, Table 1). Thus, severe torrefaction conditions would favor such decomposition.

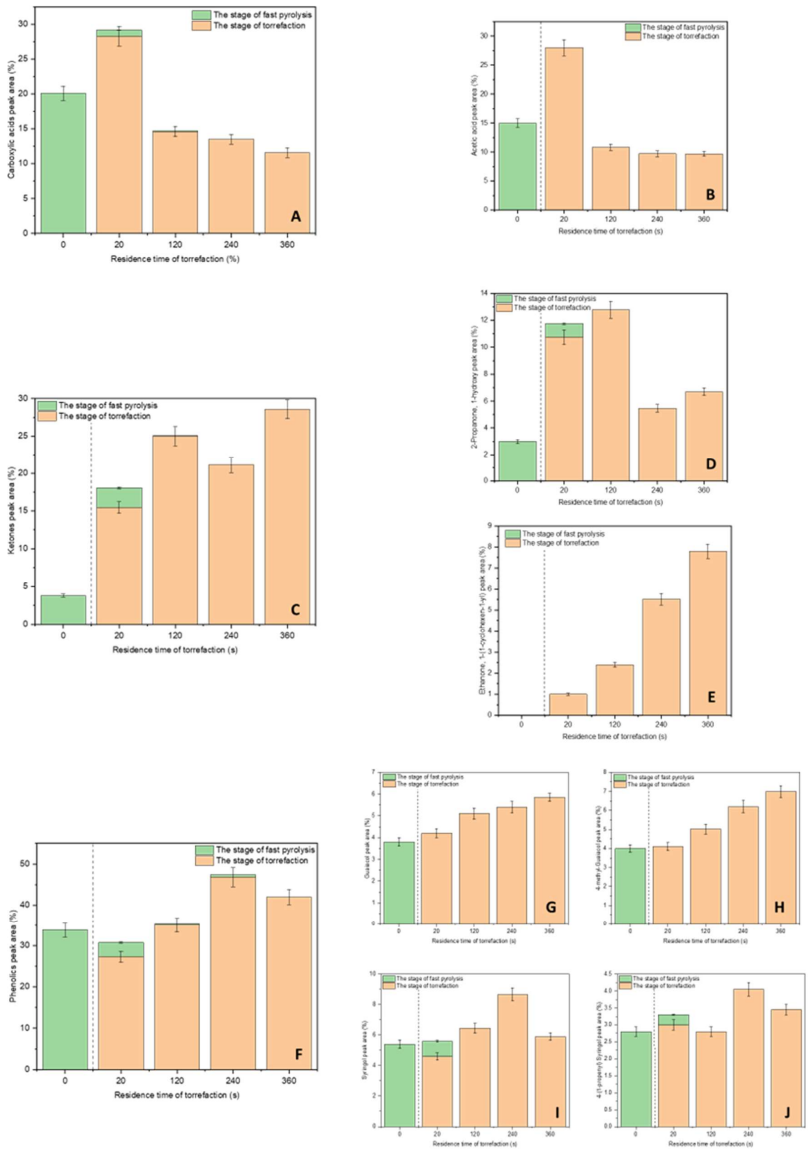

Figure 4. Bio-oil product composition for torrefaction at 320 °C and fast pyrolysis of OP. (**A**): yield of the sum of carboxylic acids, (**B**): yield of acetic acid, (**C**): yield of the sum of ketones, (**D**): yield of 2-propanone-1-hydroxy, (**E**): yield of ethanone, 1-(1-cyclohexen-1-yl), (**F**): yield of the sum of phenolics, (**G**): yield of Guaiacol, (**H**): yield of 4-methyl Guaiacol, (**I**): yield of Syringol, and (**J**): yield of 4-(1-propenyl) Syringol.

Comentado [M28]: The contents of this figure are not legible. In order to convert a clear PDF document, whilst retaining its high quality, we kindly request the provision of figures and schemes at a sufficiently high resolution (min. 1000 pixels width/height, or a resolution of 300 dpi or higher).

Comentado [ÁAR29R28]: I has been provided

3.2. Almond Shell Torrefaction Combined with Fast Pyrolysis

Figures 5–7 show bio-oil product composition for AS at different torrefaction residence times when torrefaction temperature was set at 280, 300, and 320 °C, respectively, followed by fast pyrolysis at 500 °C. Direct fast pyrolysis of AS at 500 °C (AS-500) is denoted with a torrefaction residence time of 0. The product distributions obtained were separated in the same functional groups as previously cited for OP. Tables S4–S6 give a detailed analysis of the chemical composition of bio-oil products obtained.

Direct fast pyrolysis product distribution at 500 °C for AS was mainly based on oxygenated compounds, where phenols were the most representative group, with a yield of 50.4%. The catalytic effect of AS mineral components (see Table 1) favored the formation of oxygenate compounds, such as phenolics [2]. As shown in Table 3, phenolic distribution for AS-500 was 18.3% for G-Type and 27.2% for S-Type compounds. C-type phenolic compounds were not detected by AS degradation. However, carboxylic acids were largely obtained, with *acetic acid* (the only carboxylic compound detected) reaching a yield of 28.2%. This was related to the chemical composition of AS [31,37], especially because of the amount of hemicellulose found in this biomass (28.1 wt.%). Ketones were obtained with a yield of 14.8%, with *2-Propanone*, *1-hydroxy* (5%) and *3,5-Dimethoxyacetophenone* (8.45%) being the most represented. The other compounds detected had a low molecular weight, as their production was promoted by the catalytic action of AAEMs through retro-aldol, retro Diels-Alder, or tautomerization reactions, especially when K and Ca were combined [41–43].

Table 3. Bio-oil phenolic compounds distribution of torrefied and fast pyrolysis for AS.

Sample	Peak Area (%)				
	Total Phenols	P-Type	C-Type	G-Type	S-Type
AS-500	50.4	3.7	0.0	18.3	27.2
AS-280-20	38.1	0.0	0.0	22.2	15.9
AS-280-120	36.3	0.0	0.0	12.9	22.8
AS-280-240	53.3	0.0	0.0	24.4	19.8
AS-280-360	44.9	0.0	0.0	19.8	23.3
AS-300-20	35.7	0.0	0.0	17.2	18.5
AS-300-120	40.6	0.0	0.0	20.7	18.1
AS-300-240	39.6	0.0	0.0	18.5	16.9
AS-300-360	37.4	0.0	0.0	16.9	18.3
AS-320-20	34.2	0.0	0.0	11.4	19.7
AS-320-120	32.1	2.0	0.0	14.9	13.7
AS-320-240	33.1	3.4	0.0	10.6	17.4
AS-320-360	35.3	3.2	0.0	17.4	12.5

The impact of previous torrefaction combined with fast pyrolysis of AS was studied for the following products: carboxylic acids (*Acetic acid* as the most representative compound), ketones (*2-propanone-1-hydroxy* and *3,5-Dimethoxyacetophenone* were selected as the most representative compounds produced), and lignin derivates, *Guaiacol*, *4-methyl Guaiacol*, *Syringol*, and *4-(1-propenyl) Syringol*.

At a torrefaction temperature of 280 °C (Figure 5), most of the products were mainly detected during fast pyrolysis. Only with high torrefaction residence times (generally more than 240 s) did torrefaction start to yield compounds. In contrast to OP, it seemed thermal degradation of AS was harder during torrefaction. Production of carboxylic acids was enhanced by torrefaction pretreatment at low residence times (Figure 5A), from a yield of 28.2% for AS-500 to 35.5% for AS-280-120. Yields then decreased at higher residence times. This was attributed to a significant reduction in the O-acetyl groups derived from hemicellulose [40], which were available. The main acid produced was *acetic acid*, as observed in Figure 5B. Ketone formation was also promoted, producing yields above 20%. As shown in Figure 5C,E, ketone production was enhanced during torrefaction at

residence times above 240 s, mainly due to the formation of *3,5-Dimethoxyacetophenone*. This could be interesting, as it is a phytochemical with strong pharmacological actions, such as antimicrobial and antioxidant activities. Additionally, it should be stressed that this process could be potentially considered as a source of high-quality raw materials for food and the pharmaceutical industries [30]. Regarding phenolic compounds, production was enhanced with direct fast pyrolysis (Figure 5F). If there is previous torrefaction, high residence times are required to have yields of phenolic compounds similar to that seen in AS-500. In comparison to OP, AS has a lower proportion of lignin (Table 1), which hinders its degradation into phenolics. However, changes in the distribution of the phenols obtained were observed. Thus, at high residence times, *Guaiacol* was not obtained (Figure 5G), whereas the production of *4-methyl Guaiacol* (Figure 5H) and *4-(1-propenyl) Syringol* (Figure 5J) was strongly enhanced.

At a torrefaction temperature of 300 °C (Figure 6), similar trends to those at 280 °C were observed. However, the higher temperature enabled products to be obtained during torrefaction at lower residence times. Regarding carboxylic acids, their production was again favored at low residence times (Figure 6A), with acetic acid being the most important. Ketone production (Figure 6C) gradually increased with torrefaction residence time, mainly due to the promotion of *3,5-Dimethoxyacetophenone* (Figure 6E). A combination of ketones was observed depending on the stage; *2-propanone-1-hydroxy* was only obtained during fast pyrolysis, with a clear downward trend as torrefaction residence time increased. In addition, *3,5-Dimethoxyacetophenone* formation increased with residence time and was obtained during torrefaction. Regarding phenols (Figure 6F), very similar trends as those seen at a temperature of 280 °C were observed; lower formation than with direct pyrolysis and a progressive contribution of torrefaction with residence time. *Guaiacol* (Figure 6G) was slightly promoted at low residence times, but again suppressed with higher times; while *4-methyl Guaiacol* formation (Figure 6H) improved at high residence times. Production of *4-(1-propenyl) Syringol* also improved with residence time, but the influence of torrefaction was much lower than at a temperature of 280 °C.

Finally, the results for a torrefaction temperature of 320 °C followed by fast pyrolysis at 500 °C are given in Figure 7. In short, to avoid reiterating information unnecessarily, the general trends commented on above for every group were confirmed. Additionally, production of interesting compounds such as *acid acetic*, *2-propanone-1-hydroxy*, *3,5-Dimethoxyacetophenone*, as well as phenolic types, followed the same trends already discussed. Curiously, as can be seen in Table 3, P-Type phenolics were first detected at this temperature at high residence times.

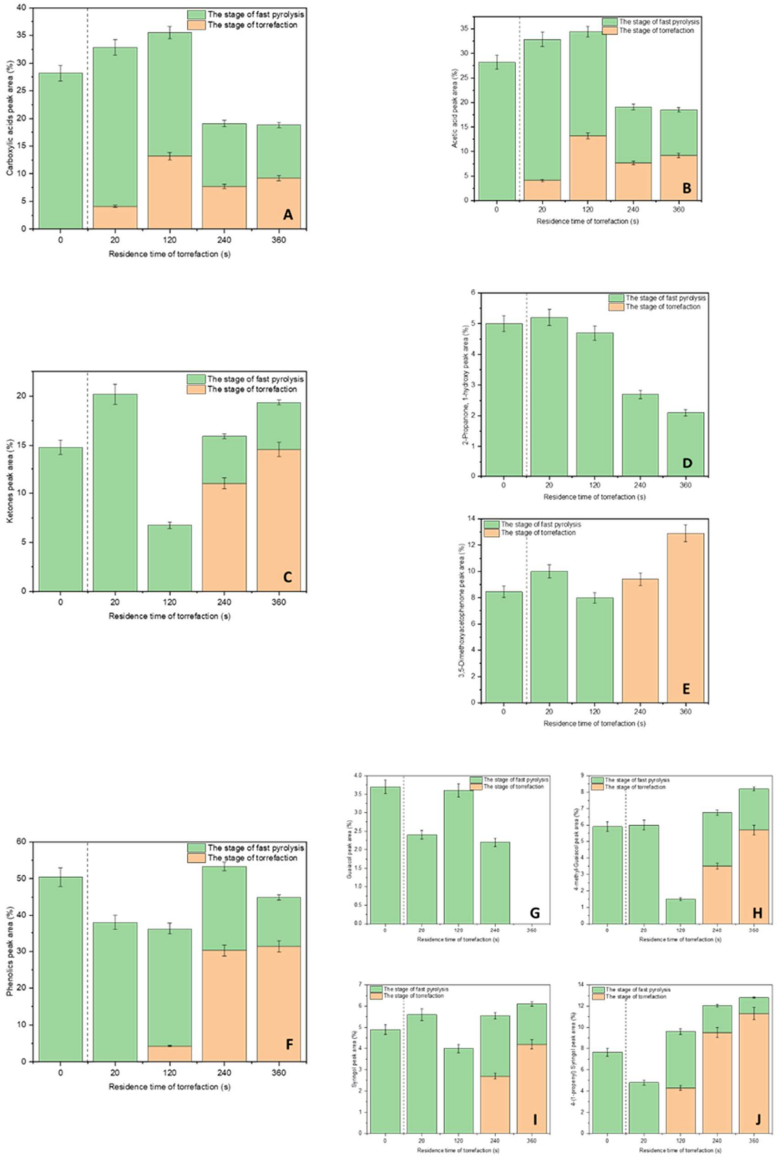

Figure 5. Bio-oil product composition for torrefaction at 280 °C and fast pyrolysis of AS. (**A**): yield of the sum of carboxylic acids, (**B**): yield of acetic acid, (**C**): yield of the sum of ketones, (**D**): yield of 2-propanone-1-hydroxy, (**E**): yield of 3,5-Dimethoxyacetophenone, (**F**): yield of the sum of phenolics, (**G**): yield of Guaiacol, (**H**): yield of 4-methyl Guaiacol, (**I**): yield of Syringol, and (**J**): yield of 4-(1-propenyl) Syringol.

Comentado [M30]: Please provide a clearer picture.

Comentado [ÁAR31R30]: I has been provided

3.3. General Trends for Combined Procedure: Torrefaction and Fast Pyrolysis

The results detailed above showed the low thermal stability of OP, so it could be completely degraded during torrefaction. This did not occur with AS, where most of the compounds were formed during the second stage: fast pyrolysis. In that case, it could be observed that cellulose and lignin rates of OP were largely decomposed during the first stage: torrefaction. With latter biomass, torrefaction pretreatment enhanced production yields. It was known that increasing torrefaction temperature and residence time could mitigate the production of volatiles and increase yields at the pyrolysis stage [40]. These observed discrepancies could be related to its physicochemical and chemical inner composition (Table 1). Therefore, it was reported that the bio-oil yield from biomass pyrolysis was reduced after it underwent torrefaction.

The compounds obtained could have been related to the organic matrix of biomass and the torrefaction conditions. During torrefaction, hemicellulose, which has poor thermal stability, decomposed first, and its content suddenly decreased with torrefaction temperature. Cellulose, which has a relatively stable structure, exhibited marginal decomposition during high-temperature torrefaction [32]. However, the lignin structure was more stable and, as a result mainly degraded during the pyrolysis stage. Production of carboxylic acids increased at low torrefaction residence times but fell sharply with high ones. The analysis suggests that O-acetyl and pentose units contained in hemicellulose are thermally degraded into acetic acid at low torrefaction residence time experiments, so acetic acid contents significantly decrease in the pyrolysis of torrefied samples [10]. Ketones were clearly promoted in comparison to direct fast pyrolysis for both biomasses, and were further enhanced at a mild torrefaction temperature (300 °C). Regarding phenolic compounds, production was closely related to the lignin content in the biomass. After torrefaction pretreatment, most of the C-C bonds within and between the alkyl chains in the lignin become unstable and reactive, causing more fragmentation to release -H, -OH, -CH_3, and -COOH in the second stage [10]. It clearly increased with OP, with a higher lignin content (24.1 wt.%) than in AS (13.4 wt.%). An increase in the torrefaction temperature intensifies the proportions of Guaiacol (*Phenol 2-methoxy*) and Syringol (*Phenol 2,6-dimethoxy*). Furthermore, the presence of inherent metals (Table 1), especially potassium, promoted dehydration and demethoxylation reactions of lignin. This produced more phenolic compounds. The presence of potassium was much higher with OP (1.46 wt.%) than with AS (0.87 wt.%). Consequently, maximum yields were obtained with OP at high torrefaction temperatures and residence times. This suggests that severe torrefaction operational conditions have a significant influence on lignin pyrolysis, and that the pyrolysis of torrefied samples results in an increase in phenolic compounds. Likewise, value-added phenolic compounds, such as *guaiacol* and *syringol*, were largely enhanced for this biomass and under these more severe torrefaction conditions. Overall, these observations are qualitatively in line with the obtained results of the Py-GC/MS in this work.

Comentado [M32]: Please confirm if the italics is unnecessary and can be removed. The following highlights are the same

Comentado [ÁAR33R32]: I Confirm

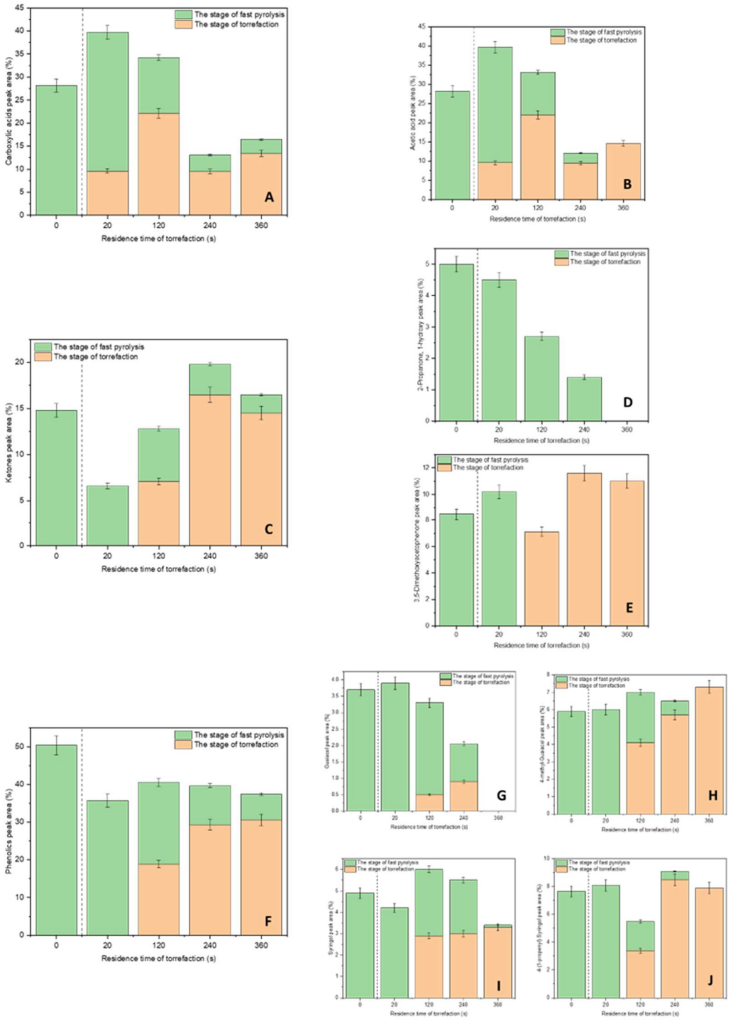

Figure 6. Bio-oil product composition for torrefaction at 300 °C and fast pyrolysis of AS. (**A**): yield of the sum of carboxylic acids, (**B**): yield of acetic acid, (**C**): yield of the sum of ketones, (**D**): yield of 2-propanone-1-hydroxy, (**E**): yield of 3,5-Dimethoxyacetophenone, (**F**): yield of the sum of phenolics, (**G**): yield of Guaiacol, (**H**): yield of 4-methyl Guaiacol, (**I**): yield of Syringol, and (**J**): yield of 4-(1-propenyl) Syringol.

Comentado [M34]: Please provide a clearer picture.

Comentado [ÁAR35R34]: I has been provided

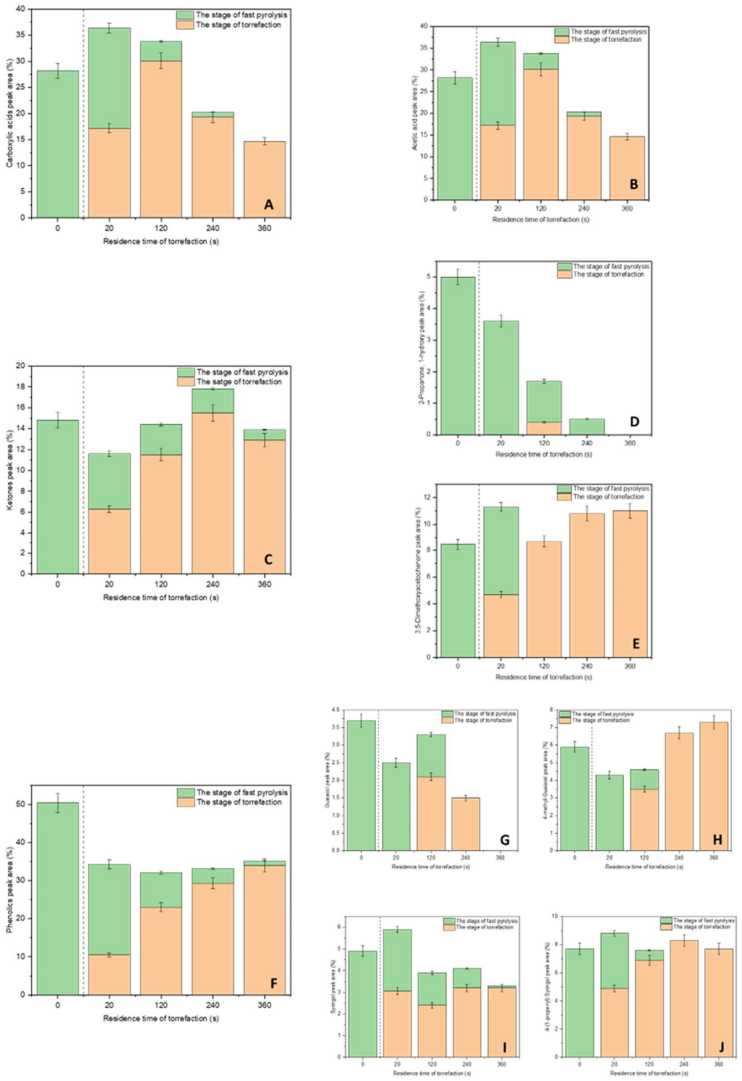

Figure 7. Bio-oil product composition for torrefaction at 320 °C and fast pyrolysis of AS. (**A**): yield of the sum of carboxylic acids, (**B**): yield of acetic acid, (**C**): yield of the sum of ketones, (**D**): yield of 2-propanone-1-hydroxy, (**E**): yield of 3,5-Dimethoxyacetophenone, (**F**): yield of the sum of phenolics, (**G**): yield of Guaiacol, (**H**): yield of 4-methyl Guaiacol, (**I**): yield of Syringol, and (**J**): yield of 4-(1-propenyl) Syringol.

Comentado [M36]: Please provide a clearer picture.

Comentado [ÁAR37R36]: I has been provided

4. Conclusions

Both torrefaction temperature and residence time had a significant effect on yields of value-added compounds in the fast pyrolysis of bio-oil from two different agricultural

waste biomasses: olive pomace and almond shell. OP, being more thermally unstable, is largely decomposed during torrefaction. Maximum carboxylic acid production, mainly acetic acid, was obtained with OP-280-20 (33.3%) and AS-300-20 (39.7%). Regarding phenolic compounds, higher production was seen with OP (higher lignin content than in AS) at high torrefaction temperatures and residence times (47.7% yield for OP-320-240). Future studies in biomass acid impregnation could maximize the production of platform chemicals through this simple pyrolytic strategy. In conclusion, this research highlights a very simple and efficient pyrolytic procedure, which provides a thermal valorization of biomass waste into value-added chemicals.

Supplementary Materials: The following supporting information can be downloaded at: www.mdpi.com/xxx/s1, Table S1. Bio-oil product composition for torrefaction at 280 °C and fast pyrolysis of OP; Table S2. Bio-oil product composition for torrefaction at 300 °C and fast pyrolysis of OP; Table S3. Bio-oil product composition for torrefaction at 320 °C and fast pyrolysis of OP; Table S4. Bio-oil product composition for torrefaction at 280 °C and fast pyrolysis of AS; Table S5. Bio-oil product composition for torrefaction at 300 °C and fast pyrolysis of AS; Table S6. Bio-oil product composition for torrefaction at 320 °C and fast pyrolysis of AS.

Author Contributions: Conceptualization, A.A.-R.; Methodology, A.A.-R. and F.D.; Investigation, A.A.-R.; Writing—original draft, A.A.-R.; Data curation, A.A.-R.; Validation, L.S.-S.; Format analysis, F.D.; Writing—review and editing. F.D. and L.S.-S.; Supervision, F.D. and L.S.-S. All authors have read and agreed to the published version of the manuscript.

Funding: This research received no external funding.

Data Availability Statement:

Conflicts of Interest: The authors declare no conflict of interest.

Comentado [M38]: In this section, please provide details regarding where data supporting reported results can be found, including links to publicly archived datasets analyzed or generated during the study. Please refer to suggested Data Availability Statements in section "MDPI Research Data Policies" at https://www.mdpi.com/ethics. You might choose to exclude this statement if the study did not report any data.

Comentado [ÁAR39R38]: I choose to exclude this statment

References

1. Jiang, C.; Jin, X.; Xu, T.; Xiao, B.; Hu, Z.; Wang, X. Biomass Chemical Looping Gasification for Syngas Production Using Modified Hematite as Oxygen Carriers. *J. Environ. Sci.* **2023**, *125*, 171–184. https://doi.org/10.1016/J.JES.2021.11.028.
2. Khan, S.R.; Zeeshan, M. Catalytic Potential of Low-Cost Natural Zeolite and Influence of Various Pretreatments of Biomass on Pyro-Oil up-Gradation during Co-Pyrolysis with Scrap Rubber Tires. *Energy* **2022**, *238*, 121820. https://doi.org/10.1016/J.ENERGY.2021.121820.
3. Kumar, A.; Kumar, K.; Kaushik, N.; Sharma, S.; Mishra, S. Renewable Energy in India: Current Status and Future Potentials. *Renew. Sustain. Energy Rev.* **2010**, *14*, 2434–2442. https://doi.org/10.1016/J.RSER.2010.04.003.
4. Zheng, A.; Xia, S.; Cao, F.; Liu, S.; Yang, X.; Zhao, Z.; Tian, Y.; Li, H. Directional Valorization of Eucalyptus Waste into Value-Added Chemicals by a Novel Two-Staged Controllable Pyrolysis Process. *Chem. Eng. J.* **2021**, *404*, 127045. https://doi.org/10.1016/j.cej.2020.127045.
5. Bridgwater, A.V.; Meier, D.; Radlein, D. An Overview of Fast Pyrolysis of Biomass. *Org. Geochem.* **1999**, *30*, 1479–1493. https://doi.org/10.1016/S0146-6380(99)00120-5.
6. Hu, R.; Wan, S.Q.; Mao, F.; Wang, J. Changes in Pyrolysis Characteristics of Agricultural Residues before and after Water Washing. *J. Fuel Chem. Technol.* **2021**, *49*, 1239–1249. https://doi.org/10.1016/S1872-5813(21)60073-7.
7. Lee, Y.E.; Jeong, Y.; Shin, D.C.; Yoo, Y.S.; Ahn, K.H.; Jung, J.; Kim, I.T. Effects of Demineralization on Food Waste Biochar for Co-Firing: Behaviors of Alkali and Alkaline Earth Metals and Chlorine. *Waste Manag.* **2022**, *137*, 190–199. https://doi.org/10.1016/j.wasman.2021.10.040.
8. Dorado, F.; Sanchez, P.; Alcazar-Ruiz, A.; Sanchez-Silva, L. Fast Pyrolysis as an Alternative to the Valorization of Olive Mill Wastes. *J. Sci. Food Agric.* **2020**, 101(7), 2650-2658. https://doi.org/10.1002/jsfa.10856.
9. González, J.F.; Ramiro, A.; González-García, C.M.; Gañán, J.; Encinar, J.M.; Sabio, E.; Rubiales, J. Pyrolysis of Almond Shells. Energy Applications of Fractions. *Ind. Eng. Chem. Res.* **2005**, *44*, 3003–3012. https://doi.org/10.1021/ie0490942.
10. Chen, W.H.; Wang, C.W.; Ong, H.C.; Show, P.L.; Hsieh, T.H. Torrefaction, Pyrolysis and Two-Stage Thermodegradation of Hemicellulose, Cellulose and Lignin. *Fuel* **2019**, *258*, 116168. https://doi.org/10.1016/j.fuel.2019.116168.
11. Chan, Y.H.; Loh, S.K.; Chin, B.L.F.; Yiin, C.L.; How, B.S.; Cheah, K.W.; Wong, M.K.; Loy, A.C.M.; Gwee, Y.L.; Lo, S.L.Y.; et al. Fractionation and Extraction of Bio-Oil for Production of Greener Fuel and Value-Added Chemicals: Recent Advances and Future Prospects. *Chem. Eng. J.* **2020**, *397*, 125406. https://doi.org/10.1016/J.CEJ.2020.125406.
12. Mohamed, B.A.; Bilal, M.; Salama, E.S.; Periyasamy, S.; Fattah, I.M.R.; Ruan, R.; Awasthi, M.K.; Leng, L. Phenolic-Rich Bio-Oil Production by Microwave Catalytic Pyrolysis of Switchgrass: Experimental Study, Life Cycle Assessment, and Economic Analysis. *J. Clean. Prod.* **2022**, *366*, 132668. https://doi.org/10.1016/J.JCLEPRO.2022.132668.
13. Li, C.; Nakagawa, Y.; Tamura, M.; Nakayama, A.; Tomishige, K. Hydrodeoxygenation of Guaiacol to Phenol over Ceria-

Comentado [M40]: Please add volume and page range/article number

Comentado [ÁAR41R40]: It has been added, as follows: "101(7):2650-2658"

Supported Iron Catalysts. *ACS Catal.* **2020**, *10*, 14624–14639. https://doi.org/10.1021/acscatal.0c04336.
14. Cao, B.; Jiang, D.; Zheng, Y.; Fatemeh, P.; Yuan, C.; Hu, Y.; Chen, H.; Li, C.; Hu, X.; Wang, S.; et al. Evaluation of Biochar-Derived Carbocatalysts for Pyrolytic Conversion of Sawdust : Life Cycle Assessment towards Monophenol Production. *Fuel* **2022**, *330*, 125476. https://doi.org/10.1016/j.fuel.2022.125476.
15. Chen, X.; Che, Q.; Li, S.; Liu, Z.; Yang, H.; Chen, Y.; Wang, X.; Shao, J.; Chen, H. Recent Developments in Lignocellulosic Biomass Catalytic Fast Pyrolysis: Strategies for the Optimization of Bio-Oil Quality and Yield. *Fuel Process. Technol.* **2019**, *196*, 106180. https://doi.org/10.1016/J.FUPROC.2019.106180.
16. Foong, S.Y.; Liew, R.K.; Yang, Y.; Cheng, Y.W.; Yek, P.N.Y.; Wan Mahari, W.A.; Lee, X.Y.; Han, C.S.; Vo, D.-V.N.; Van Le, Q.; et al. Valorization of Biomass Waste to Engineered Activated Biochar by Microwave Pyrolysis: Progress, Challenges, and Future Directions. *Chem. Eng. J.* **2020**, *389*, 124401. https://doi.org/10.1016/J.CEJ.2020.124401.
17. Chen, W.H.; Lin, B.J.; Lin, Y.Y.; Chu, Y.S.; Ubando, A.T.; Show, P.L.; Ong, H.C.; Chang, J.S.; Ho, S.H.; Culaba, A.B.; et al. Progress in Biomass Torrefaction: Principles, Applications and Challenges. *Prog. Energy Combust. Sci.* **2021**, *82*, 100887. https://doi.org/10.1016/J.PECS.2020.100887.
18. Louwes, A.C.; Basile, L.; Yukananto, R.; Bhagwandas, J.C.; Bramer, E.A.; Brem, G. Torrefied Biomass as Feed for Fast Pyrolysis: An Experimental Study and Chain Analysis. *Biomass Bioenergy* **2017**, *105*, 116–126. https://doi.org/10.1016/j.biombioe.2017.06.009.
19. Yue, Y.; Singh, H.; Singh, B.; Mani, S. Torrefaction of Sorghum Biomass to Improve Fuel Properties. *Bioresour. Technol.* **2017**, *232*, 372–379. https://doi.org/10.1016/J.BIORTECH.2017.02.060.
20. Zheng, A.; Zhao, Z.; Chang, S.; Huang, Z.; He, F.; Li, H. Effect of Torrefaction Temperature on Product Distribution from Two-Staged Pyrolysis of Biomass. *Energy Fuels* **2012**, *26*, 2968–2974. https://doi.org/10.1021/ef201872y.
21. Nepal, R.; Kim, H.J.; Poudel, J.; Oh, S.C. A Study on Torrefaction of Spent Coffee Ground to Improve Its Fuel Properties. *Fuel* **2022**, *318*, 123643. https://doi.org/10.1016/J.FUEL.2022.123643.
22. Dai, L.; Wang, Y.; Liu, Y.; Ruan, R.; He, C.; Yu, Z.; Jiang, L.; Zeng, Z.; Tian, X. Integrated Process of Lignocellulosic Biomass Torrefaction and Pyrolysis for Upgrading Bio-Oil Production: A State-of-the-Art Review. *Renew. Sustain. Energy Rev.* **2019**, *107*, 20–36. https://doi.org/10.1016/J.RSER.2019.02.015.
23. Qian, X.; Lee, S.; Soto, A.M.; Chen, G. Regression Model to Predict the Higher Heating Value of Poultry Waste from Proximate Analysis. *Resources* **2018**, *7*, 39. https://doi.org/10.3390/resources7030039.
24. Qian, X.; Xue, J.; Yang, Y.; Lee, S.W. Thermal Properties and Combustion-related Problems Prediction of Agricultural Crop Residues. *Energies* **2021**, *14*, 4619. https://doi.org/10.3390/en14154619.
25. Kan, T.; Strezov, V.; Evans, T.J. Lignocellulosic Biomass Pyrolysis: A Review of Product Properties and Effects of Pyrolysis Parameters. *Renew. Sustain. Energy Rev.* **2016**, *57*, 1126–1140. https://doi.org/10.1016/J.RSER.2015.12.185.
26. TAPPI. *TAPPI/ANSI Test Method T 401 Om-15-Fiber Analysis of Paper and Paperboard*; 2018 (Nocross, Atlanta, USA); ISBN 7704461400.
27. López-González, D.; Fernandez-Lopez, M.; Valverde, J.L.; Sanchez-Silva, L. Thermogravimetric-Mass Spectrometric Analysis on Combustion of Lignocellulosic Biomass. *Bioresour. Technol.* **2013**, *143*, 562–574. https://doi.org/10.1016/J.BIORTECH.2013.06.052.
28. Miranda, I.; Simões, R.; Medeiros, B.; Nampoothiri, K.M.; Sukumaran, R.K.; Rajan, D.; Pereira, H.; Ferreira-Dias, S. Valorization of Lignocellulosic Residues from the Olive Oil Industry by Production of Lignin, Glucose and Functional Sugars. *Bioresour. Technol.* **2019**, *292*, 121936. https://doi.org/10.1016/J.BIORTECH.2019.121936.
29. Chen, D.; Cen, K.; Chen, F.; Zhang, Y. Solar Pyrolysis of Cotton Stalks: Combined Effects of Torrefaction Pretreatment and HZSM-5 Zeolite on the Bio-Fuels Upgradation. *Energy Convers. Manag.* **2022**, *261*, 115640. https://doi.org/10.1016/J.ENCONMAN.2022.115640.
30. Alghamdi, S.S.; Khan, M.A.; El-Harty, E.H.; Ammar, M.H.; Farooq, M.; Migdadi, H.M. Comparative Phytochemical Profiling of Different Soybean (*Glycine max* (L.) Merr) Genotypes Using GC–MS. *Saudi J. Biol. Sci.* **2018**, *25*, 15–21. https://doi.org/10.1016/J.SJBS.2017.10.014.
31. Alcazar-Ruiz, A.; Garcia-Carpintero, R.; Dorado, F.; Sanchez- Silva, L. Valorization of Olive Oil Industry Subproducts: Ash and Olive Pomace Fast Pyrolysis. *Food Bioprod. Process.* **2021**, *125*, 37–45. https://doi.org/10.1016/j.fbp.2020.10.011.
32. Huang, M.; Ma, Z.; Zhou, B.; Yang, Y.; Chen, D. Enhancement of the Production of Bio-Aromatics from Renewable Lignin by Combined Approach of Torrefaction Deoxygenation Pretreatment and Shape Selective Catalytic Fast Pyrolysis Using Metal Modified Zeolites. *Bioresour. Technol.* **2020**, *301*, 122754. https://doi.org/10.1016/j.biortech.2020.122754.
33. Huang, M.; Xu, J.; Ma, Z.; Yang, Y.; Zhou, B.; Wu, C.; Ye, J.; Zhao, C.; Liu, X.; Chen, D.; et al. Bio-BTX Production from the Shape Selective Catalytic Fast Pyrolysis of Lignin Using Different Zeolite Catalysts: Relevance between the Chemical Structure and the Yield of Bio-BTX. *Fuel Process. Technol.* **2021**, *216*, 106792. https://doi.org/10.1016/j.fuproc.2021.106792.
34. Torres, D.; Pérez-Rodríguez, S.; Cesari, L.; Castel, C.; Favre, E.; Fierro, V.; Celzard, A. Review on the Preparation of Carbon Membranes Derived from Phenolic Resins for Gas Separation: From Petrochemical Precursors to Bioresources. *Carbon* **2021**, *183*, 12–33. https://doi.org/10.1016/J.CARBON.2021.06.087.
35. Huang, C.; Zhan, Y.; Cheng, J.; Wang, J.; Meng, X.; Zhou, X.; Fang, G.; Ragauskas, A.J. Facilitating Enzymatic Hydrolysis with a Novel Guaiacol-Based Deep Eutectic Solvent Pretreatment. *Bioresour. Technol.* **2021**, *326*, 124696. https://doi.org/10.1016/J.BIORTECH.2021.124696.
36. Curmi, H.; Chirat, C.; Roubaud, A.; Peyrot, M.; Haarlemmer, G.; Lachenal, D. Extraction of Phenolic Compounds from Sulfur-Free Black Liquor Thanks to Hydrothermal Treatment before the Production of Syngas for Biofuels. *J. Supercrit. Fluids* **2022**, *181*,

Comentado [M42]: Please add publisher and location (city, country)

Comentado [ÁAR43R42]: It has been added

Comentado [M44]: Newly added information. Please confirm.

Comentado [ÁAR45R44]: I Confirm

105489. https://doi.org/10.1016/j.supflu.2021.105489.
37. Oh, S.J.; Choi, G.G.; Kim, J.S. Production of Acetic Acid-Rich Bio-Oils from the Fast Pyrolysis of Biomass and Synthesis of Calcium Magnesium Acetate Deicer. *J. Anal. Appl. Pyrolysis* **2017**, *124*, 122–129. https://doi.org/10.1016/j.jaap.2017.01.032.
38. Chagas, B.M.E.; Dorado, C.; Serapiglia, M.J.; Mullen, C.A.; Boateng, A.A.; Melo, M.A.F.; Ataíde, C.H. Catalytic Pyrolysis-GC/MS of Spirulina: Evaluation of a Highly Proteinaceous Biomass Source for Production of Fuels and Chemicals. *Fuel* **2016**, *179*, 124–134. https://doi.org/10.1016/J.FUEL.2016.03.076.
39. Schmeltz, I.; Schlotzhauer, W.S.; Higman, E.B. Characteristic Products from Pyrolysis of Nitrogenous Organic Substances. *Beiträge Zur Tab. Int. Contrib. Tob. Nicotine Res.* **1972**, *6*, 134–138. https://doi.org/10.2478/cttr-2013-0281.
40. Valizadeh, S.; Oh, D.; Jae, J.; Pyo, S.; Jang, H.; Yim, H.; Rhee, G.H.; Khan, M.A.; Jeon, B.H.; Lin, K.Y.A.; et al. Effect of Torrefaction and Fractional Condensation on the Quality of Bio-Oil from Biomass Pyrolysis for Fuel Applications. *Fuel* **2022**, *312*, 122959. https://doi.org/10.1016/j.fuel.2021.122959.
41. Alcazar-Ruiz, A.; Ortiz, M.L.; Sanchez-Silva, L.; Dorado, F. Catalytic Effect of Alkali and Alkaline Earth Metals on Fast Pyrolysis Pre-Treatment of Agricultural Waste. *Biofuels Bioprod. Biorefining* **2021**, *15*, 1473–1484. https://doi.org/10.1002/bbb.2253.
42. Fermoso, J.; Hernando, H.; Jana, P.; Moreno, I.; Přech, J.; Ochoa-Hernández, C.; Pizarro, P.; Coronado, J.M.; Čejka, J.; Serrano, D.P. Lamellar and Pillared ZSM-5 Zeolites Modified with MgO and ZnO for Catalytic Fast-Pyrolysis of Eucalyptus Woodchips. *Catal. Today* **2016**, *277*, 171–181. https://doi.org/10.1016/j.cattod.2015.12.009.
43. Zhou, X.; Nolte, M.W.; Shanks, B.H.; Broadbelt, L.J. Experimental and Mechanistic Modeling of Fast Pyrolysis of Neat Glucose-Based Carbohydrates. 2. Validation and Evaluation of the Mechanistic Model. *Ind. Eng. Chem. Res.* **2014**, *53*, 13290–13301. https://doi.org/10.1021/ie502260q.

Comentado [M46]: Newly added information. Please confirm.

Comentado [ÁAR47R46]: I Confirm

Comentado [M48]: Newly added information. Please confirm.

Comentado [ÁAR49R48]: I Confirm